

# Sensitivity of Dynamics of *Toxoplasma gondii* and Host Immune Response

Avinita Gautam<sup>1\*</sup> and Anupam Priyadarshi<sup>2</sup>

<sup>1</sup> DST-CIMS, Institute of Science, Banaras Hindu University, Varanasi, India  
(E-mail: [avinita.gautam2@bhu.ac.in](mailto:avinita.gautam2@bhu.ac.in))

<sup>2</sup> Department of Mathematics, Institute of Science, Banaras Hindu University, Varanasi, India  
(E-mail: [anupam240@gmail.com](mailto:anupam240@gmail.com))

**Abstract.** Epidemiology is essential to understand the reason of spreading the disease, its outburst and control of the various diseases. Toxoplasmosis is a protozoan parasite that can infect all warm blood vertebrates, including mammals and birds. Approximately 20% human population in US and 30% world-wide are infected by protozoan parasite. It is happen mainly due to single cell parasite *T. gondii*. The present study exhibits the mathematical modeling of interaction between *Toxoplasma gondii* invasion dynamics and host immune responses through simple ODE system. To observe the impact of parameters on the reproduction number, sensitivity analysis has been done. The analytic and numerical simulations are carried out to understand that the impact of Holling type II functional response and observed that it enhanced the effector cells of host's immune response.

**Keywords:** *Toxoplasma gondii*, neurological disorders, sensitivity, immune system.

## 1 Introduction

Epidemiological and immunological processes in host-parasite interactions are two main key factors for infectious diseases [1]. Epidemiological models developed by considering interactions between susceptible and infected class of host population which does not depend on within-host dynamics [1]. Within-host dynamics affect the viral dynamics models in which interactions of different classes of host populations does not play any role. One third of the world human populations are infected depending on exposure to cats and eating habits [2]. Life cycle of infection due to *Toxoplasma gondii* can be understood by figure 1.

*Toxoplasma gondii* is most common insidious parasite which works as intermediate hosts and infects wide range of mammals [3]. It is a causative protozoan which is responsible for most common zoonosis 'Toxoplasmosis' [3]. Studies suggest that *Toxoplasma* infection may cause chronic neurological disorders [4]. *T. Gondii* elevates the concentration of chemicals in neurotransmitter and causes brain infection [5]. Multiplication of parasites in central nervous system also causes neurological disorders and sometimes it may also cause brain damage

---

Received: 15 November 2020 / Accepted: 16 April 2021

© 2021 CMSIM



ISSN 2241-0503

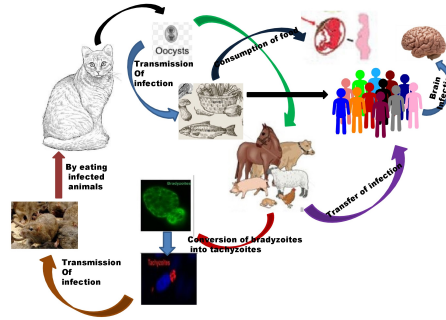


**Fig. 1.** Life cycle of *Toxoplasma gondii* including brain infection

[2]. From the recent studies it has been found that *T. gondii* infection causes behavioral alteration [6,7] in hosts and neurological disorders like schizophrenia or bipolar disorders etc. [2,8,9]. Immune responses in the brain play a vital role in persistence of *T. gondii* cysts [5] and when immune get stimulated *T. gondii* causes local inflammatory. Toxoplasmosis can affect the fetal brain development and it may cause alteration of brain activity. The causative agent of Toxoplasmosis can dominate the neural activity of hosts and may change its behavior or function [6]. There are two types of infection due to *T. gondii* - one is congenital and second is acquired form [2]. Consumption of contaminated water, undercooked meats and raw vegetable potential risk factors for infection due to *Toxoplasma gondii* from where humans acquire infection [2,3]. Generally the lifecycle of *T. gondii* contain three stages-oocytes, bradyzoites and tachyzoites [3,10]. Climates also play an important role in maturation and transmission of oocytes in new hosts as it faster processed in wet climates [2]. Abortion and many malformations of fetus or neurological disorders occur when a pregnant woman acquires congenital Toxoplasmosis for the first time during pregnancy [2]. Mammals having weak immune system can easily get infected by toxoplasmosis and may have serious implication of brain [11].

## 2 Mathematical Model

Let us considered  $X$  as a population size of uninfected cells,  $Y_T$  as a population of cells infected with tachyzoites,  $Y_B$  as a population of cells containing early-stage bradyzoites,  $Y_C$  as a population of cells containing encysted bradyzoites. Now let us assume that  $P_T$  is the population of free tachyzoites  $P_B$  is the population of free bradyzoites,  $Z$  is the effector cells of the host's immune response. Let us suppose  $\lambda$  is growth rate of uninfected cell,  $\frac{1}{d}$  is the average life time of an uninfected cell. If there is no infection in host cells then the dynamics of host cells can be expressed by

$$\frac{dx}{dt} = \lambda - dX; \quad (1)$$

It shows that the uninfected cells converge to equilibrium point  $X_0$ , which is given by  $X_0 = \frac{\lambda}{d}$ . However, in case of infection there are many situations which

will be discussed mathematically that how free parasites infect uninfected host cells and other conversion stages of infections. Let  $\beta_{PT}$  and  $\beta_{PB}$  are rate constants,  $\frac{1}{a_T}$  is the average life time of a cell infected with tachyzoites,  $\frac{1}{a_C}$  is the average life time of a cell infected with bradyzoites,  $k_T$  is the production rate of free parasite for tachyzoites,  $k_C$  is the production rate of free parasite for bradyzoites,  $u_T$  is the removal rate of free parasite for tachyzoites,  $u_B$  is the removal rate of free parasite for bradyzoites,  $\delta$  is the removal rate of the immune system response,  $\rho$  is the production rate of the effector cells,  $c_T$  is efficiency rate constant,  $h$  is half saturation constant,  $r_B$  is the rate of conversion of early-stage bradyzoites,  $r_T$  is the rate of conversion of Tachyzoites. This model includes invasion process; inter conversion between two stages bradyzoites and tachyzoites and host's immune response and whole dynamics can be easily shown by the flowing flow diagram as follows:

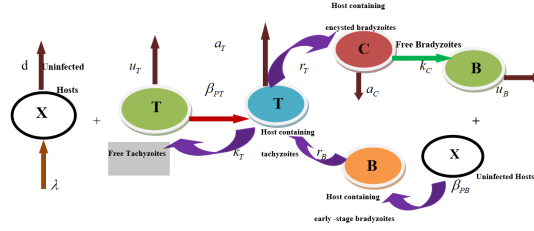


Fig. 2. Compartment Model of dynamics of Toxoplasma gondii

Also, the whole dynamics of *T. gondii* of above compartmental model (Fig.2) can be expressed mathematically by the following model 1(a) given by the equations (2-8):

$$\frac{dX}{dt} = dX\left(1 - \frac{X}{X_0}\right) - \beta_{PT}XP_T - \beta_{PB}XP_B \tag{2}$$

$$\frac{dY_T}{dt} = \beta_{PT}XP_T - a_TY_T - r_TY_T + r_BY_B - \frac{c_TY_TZ}{h + Y_T} \tag{3}$$

$$\frac{dY_C}{dt} = r_TY_T - a_CY_C \tag{4}$$

$$\frac{dY_B}{dt} = \beta_{PB}XP_B - r_BY_B \tag{5}$$

$$\frac{dP_T}{dt} = k_TY_T - u_TP_T \tag{6}$$

$$\frac{dP_B}{dt} = k_CY_C - u_BP_B \tag{7}$$

$$\frac{dZ}{dt} = \frac{\rho Y_T Z}{h + Y_T} - \delta Z \quad (8)$$

Here, free parasites are considered in equilibrium state so by equating eqn. (6) and eqn. (7) of model (1a) to zero, we have

$$P_T = \frac{k_T Y_T}{u_T}; \quad P_B = \frac{k_C Y_C}{u_B} \quad (9)$$

Now substituting the above values of  $P_T$  and  $P_B$  in equations set of model 1(a), we get following expression as a model 1(b) given by equation (10 -14):

$$\frac{dX}{dt} = dX \left(1 - \frac{X}{X_0}\right) - \beta_T X Y_T - \beta_B X Y_C \quad (10)$$

$$\frac{dY_T}{dt} = \beta_T X Y_T - a_T Y_T - r_T Y_T + r_B Y_B - \frac{c_T Y_T Z}{h + Y_T} \quad (11)$$

$$\frac{dY_C}{dt} = r_T Y_T - a_C Y_C \quad (12)$$

$$\frac{dY_B}{dt} = \beta_B X Y_C - r_B Y_B \quad (13)$$

$$\frac{dZ}{dt} = \frac{\rho Y_T Z}{h + Y_T} - \delta Z \quad (14)$$

where

$$\beta_T = \frac{k_T \beta_{PT}}{u_T}; \quad \beta_B = \frac{k_C \beta_{PB}}{u_B} \quad (15)$$

### 3 Stability Analysis

#### 3.1 Disease-Free Equilibrium (DFE)

The equations of model 1(b) implies there exists a unique non-negative DFE solution. Denote this equilibrium solution by  $E_0 = (X_0, 0, 0, 0, 0)$ . Let  $F$  be matrix of the rates of new infection and  $V$  is the matrix of rates of infection due to transmission.

Now from model 1(b),

$$F = \begin{bmatrix} \beta_T X & 0 & 0 \\ 0 & 0 & 0 \\ 0 & \beta_T X & 0 \end{bmatrix} \quad (16)$$

and

$$V = \begin{bmatrix} a_T + r_T & 0 & -r_T \\ -r_T & a_C & 0 \\ 0 & 0 & r_B \end{bmatrix} \quad (17)$$

It follows that the basic reproduction number of equations set of model 1(b) by using next-generation method, denoted by  $R_0$ , is given by

$$R_0 = \rho(FV^{-1}) = \frac{X_0(a_C\beta_T + \beta_B r_T)}{a_C(a_T + r_T)} \quad (18)$$

where  $\rho$  is the spectral radius.

### 3.2 Endemic Equilibrium (DFE)

Let  $E_1^* = (X^*, Y_T^*, Y_C^*, Y_B^*, Z)$  be equilibrium point of the model 1(b). Let

$$\lambda_1 = Y_T\beta_T \text{ and } \lambda_2 = Y_T\beta_T \quad (19)$$

Let  $x$  be the force of infection is given by equation (20) as follows:

$$x = \lambda_1 + \lambda_2 \quad (20)$$

Firstly, endemic equilibrium has been determined in which immunity is not considered ( $Z = 0$ ). By equating right hand side of equations of model 1(b) to zero, we have the expressions in terms of  $\lambda_1$  and  $\lambda_2$  at steady state for the model 1(b) given by equations (21 - 24).

$$X^* = \frac{(d - \lambda_1^* - \lambda_2^*)X_0}{d} \quad (21)$$

$$Y_T^* = \frac{(d - \lambda_1^* - \lambda_2^*)(\lambda_1^* + \lambda_2^*)}{d(a_T + r_T)} \quad (22)$$

$$Y_B^* = \frac{(d - \lambda_1^* - \lambda_2^*)X_0}{dr_B} \quad (23)$$

$$Y_C^* = \frac{X_0 r_T (d - \lambda_1^* - \lambda_2^*)(\lambda_1^* + \lambda_2^*)}{da_C(a_T + r_T)} \quad (24)$$

After the putting expressions of equations (21 - 24) in equation (20) we have the following expression for force of infection for model 1(b),

$$x = d\left(1 - \frac{1}{R_0}\right) = d\frac{(R_0 - 1)}{R_0} \quad (25)$$

Thus from the above expression it can be observed that  $x > 0$  if and only if  $R_0 > 1$ . Thus, when immune response has not been considered then model 1(b) has unique endemic equilibrium if  $R_0 > 1$ .

Next, we have considered when immunity is present in the system that is  $Z \neq 0$ . Again equating right hand side of equations of model 1(b) to zero, we will have the following set of equations (26 - 30):

$$X^* = \frac{(d - \lambda^*_1 - \lambda^*_2)X_0}{d} \quad (26)$$

$$Y_T^* = \frac{\delta h}{\rho - \delta} \quad (27)$$

$$Y_C^* = \frac{r_T \delta h}{(\rho - \delta) a_C} \quad (28)$$

$$Y_B^* = \frac{\lambda^*_2 (d - \lambda^*_1 - \lambda^*_2) X_0}{d r_B} \quad (29)$$

$$Z^* = \frac{(\lambda^*_1 - \lambda^*_2)(\rho - \delta)(d - \lambda^*_1 - \lambda^*_2)X_0 - d\delta h(a_T + r_T)}{dh\delta c_T} \quad (30)$$

After substituting the expressions of equations (26 - 30) in equation (20), we have

$$x = \frac{h\delta(a_T + r_T)(R_0 - 1)}{\rho - \delta} + \frac{h\delta(a_T + r_T)}{\rho - \delta} \quad (31)$$

Here it can be seen that the force of equation given by equation (31),  $x > 0$  if and only if and  $R_0 > 1$  and  $\rho > \delta$ . Hence the equilibrium points for model 1(b) is given by

$$E_2^* = \left( \frac{(d - \lambda^*_1 - \lambda^*_2)X_0}{d}, \frac{\delta h}{\rho - \delta}, \frac{r_T \delta h}{(\rho - \delta) a_C}, \frac{\lambda^*_2 (d - \lambda^*_1 - \lambda^*_2) X_0}{d r_B}, Z^* \right) \quad (32)$$

where  $Z^*$  is given by equation (30).

Thus, when active immune response has been considered then model 1(b) has unique endemic equilibrium if and  $R_0 > 1$  and  $\rho > \delta$ .

### 3.3 Local stability of Disease-free equilibrium

Let us consider the model 1(b) and we have the Jacobian  $J_{E_0}$  at equilibrium point  $E_0$  which is given as follows:

$$J_{E_0} = \begin{bmatrix} -d & -\beta_T X_0 & -\beta_B X_0 & 0 & 0 \\ 0 & \beta_T X_0 - (a_T + r_T) & 0 & r_B & 0 \\ 0 & r_T & -a_C & 0 & 0 \\ 0 & 0 & \beta_B X_0 & -r_B & 0 \\ 0 & 0 & 0 & 0 & -\delta \end{bmatrix} \quad (33)$$

Clearly, we have two eigenvalues as  $-d$  and  $-\delta$  and remaining three eigenvalues are obtained by the following cubic equation,

$$\lambda^3 + a\lambda^2 + b\lambda + c = 0 \quad (34)$$

Therefore, by using Routh-Hurwitz criteria we can say that equation (34) has negative real parts of eigenvalues if it satisfies the following conditions:

1.  $a > 0, b > 0, c > 0$  and
2.  $ab > c$

where

$$a = a_T + a_C - \beta_T X_0 + r_T + r_B \quad (35)$$

$$b = a_T a_C - \beta_T a_C X_0 + r_T r_B a_C - r_B \beta_T X_0 + r_T r_B + r_T a_C \quad (36)$$

$$c = a_T a_C r_B - a_C r_B \beta_T X_0 + r_T r_B a_C - r_T r_B \beta_B X_0 \quad (37)$$

Now, we can write

$$a = a_T + a_C - \beta_T X_0 + r_T + r_B \quad (38)$$

$$= a_C + r_B + \frac{r_T \beta_B X_0}{a_C} + (a_T + r_T)(1 - R_0) \quad (39)$$

$$\therefore a > 0 \text{ if } R_0 < 1$$

Again,

$$b = a_T a_C r_B - a_C r_B \beta_T X_0 + r_T r_B a_C - r_T r_B \beta_B X_0 \quad (40)$$

$$= (1 - R_0) a_C (a_T + r_T) + (1 - R_0) (a_T + r_T) r_B + a_C r_B + \frac{r_T r_B \beta_B X_0}{a_C} + r_T \beta_B X_0 \quad (41)$$

$$> 0 \text{ if } R_0 < 1$$

Also,

$$c = a_T a_C r_B - a_C r_B \beta_T X_0 + r_T r_B a_C - r_T r_B \beta_B X_0 \quad (42)$$

$$= (1 - R_0) r_B a_C (a_T + r_T) \quad (43)$$

$$> 0 \text{ if } R_0 < 1$$

This implies that, all the roots of the Jacobian matrix have negative real parts. Hence, the disease-free equilibrium of the model 1(b) is locally asymptotically stable if  $R_0 < 1$  and unstable if  $R_0 > 1$ . That is if the reproduction number  $R_0$ , reduced to less than unity then infection due to *Toxoplasma gondii* can be eliminated from the hosts.

### 3.4 Local stability of Endemic equilibrium

When immune response  $Z=0$

Let us consider the model 1(b) and we have the Jacobian  $J_{E_1^*}$  at equilibrium point  $E_1^*$  which is given as follows:

$$J_{E_1^*} = \begin{bmatrix} g_{11} & g_{12} & g_{13} & 0 \\ g_{21} & g_{22} & 0 & r_B \\ 0 & g_{32} & g_{33} & 0 \\ g_{41} & 0 & g_{43} & -r_B \end{bmatrix} \quad (44)$$

where,

$$g_{11} = d(1 - 2\frac{X^*}{X_0}) - (\beta_T Y_T^* + Y_C^* \beta_B), \quad g_{12} = -\beta_T X_0, \quad g_{13} = -\beta_B X_0, \quad g_{21} = -\beta_T Y_T^*, \\ g_{41} = -\beta_B Y_C^*, \quad g_{22} = \beta_T X_0 - (a_T + r_T), \quad g_{43} = \beta_B X_0, \quad g_{32} = r_T, \quad g_{33} = -a_C$$

Eigenvalues of the Jacobian matrix can be calculated by the following equation

$$\lambda^4 + a\lambda^3 + b\lambda^2 + c\lambda + d = 0 \quad (45)$$

where,

$$a = g_{11} - g_{22} - g_{33}, \quad b = -g_{12}g_{21} + g_{11}g_{22} + g_{33}g_{11} + g_{22}g_{33} - g_{11}\Gamma_B - g_{22}\Gamma_B - g_{33}\Gamma_B \quad (46)$$

$$c = -g_{13}g_{21}g_{32} + g_{12}g_{21}g_{33} - g_{11}g_{22}g_{33} - g_{12}g_{21}\Gamma_B + g_{11}g_{22}\Gamma_B + g_{11}g_{33}\Gamma_B + g_{22}g_{33}\Gamma_B - g_{12}g_{41}\Gamma_B - g_{32}g_{43}\Gamma_B \quad (47)$$

$$d = -g_{13}g_{21}g_{32}\Gamma_B + g_{12}g_{21}g_{33}\Gamma_B - g_{11}g_{22}g_{33}\Gamma_B - g_{13}g_{32}g_{41}\Gamma_B + g_{12}g_{33}g_{41}\Gamma_B + g_{11}g_{32}g_{43}\Gamma_B \quad (48)$$

Now by using Routh-Hurwitz criteria, we have negative real parts of eigenvalues of equation (45) if it satisfies following conditions as follows:

1.  $a > 0, b > 0, c > 0, d > 0$
2.  $ab > c$  and
3.  $abc > c^2 + a^2d$

We have obtained same results in the case of model 1(b), since immune response is not considered in this case. Thus the endemic equilibrium of the model (1b) is locally asymptotically stable in the absence of immune if  $R_0 < 1$ .

*When immune response  $Z \neq 0$*

Let us consider the model 1(b) and we have the Jacobian  $J_{E_2^*}$  at equilibrium point  $E_2^*$  which is given as follows:

$$J_{E_2^*} = \begin{bmatrix} g_{11} & g_{12} & g_{13} & 0 & 0 \\ g_{21} & g_{22} & 0 & \Gamma_B & g_{25} \\ 0 & \Gamma_T & -a_C & 0 & 0 \\ g_{41} & 0 & g_{43} & -\Gamma_B & 0 \\ 0 & g_{52} & 0 & 0 & 0 \end{bmatrix} \quad (49)$$

where,

$$g_{11} = \frac{2[(\lambda_1^* + \lambda_2^*) - d](\rho - \delta) - \beta_T a_C \delta h + \delta r_T h \beta_B}{a_C(\rho - \delta)}, \quad g_{12} = -\beta_T \frac{(d - \lambda_1^* - \lambda_2^*)X_0}{d}, \quad g_{13} = -\beta_B \frac{(d - \lambda_1^* - \lambda_2^*)X_0}{d}$$

$$g_{21} = \frac{-\beta_T h \delta}{\rho - \delta}, \quad g_{25} = -\frac{c_T \delta}{\rho}, \quad g_{41} = \frac{-\beta_B h \delta r_T}{a_C(\rho - \delta)}, \quad g_{43} = \beta_B \frac{(d - \lambda_1^* - \lambda_2^*)X_0}{d}$$

$$g_{22} = -\beta_T \frac{(d - \lambda_1^* - \lambda_2^*)X_0}{d} - (c_T + r_T) - \frac{(d - \lambda_1^* - \lambda_2^*)(\lambda_1^* - \lambda_2^*)(\rho - \delta)X_0 - dh\delta(a_T + r_T)}{d\delta c_T h}$$

$$g_{52} = \frac{(d - \lambda_1^* - \lambda_2^*)(\lambda_1^* - \lambda_2^*)(\rho - \delta)X_0 - dh\delta(a_T + r_T)(\rho - \delta)^2}{d\delta c_T h^2 \rho} (\rho - \delta)^2$$

Eigenvalues can be calculated by solving the following equation (50) given as follows:

$$\lambda^5 + a\lambda^4 + b\lambda^3 + c\lambda^2 + d\lambda + e = 0 \quad (50)$$

Now, by using Routh-Hurwitz criteria, we have negative real parts of eigenvalues of equation (50) if it satisfies following conditions as follows:

1.  $a > 0, b > 0, c > 0, d > 0$
2.  $ab > c$
3.  $abc > c^2 + a^2d$  and
4.  $abcd + 2ade + bce > a^2d^2 + e^2 + c^2d + ab^2e$

Thus the endemic equilibrium of the model (1b) is locally asymptotically stable in the presence of immune if  $R_0 < 1$  and  $\rho < \delta$ .

## 4 Numerical Analysis

In above section we proposed the model with certain assumptions and have performed stability analysis. We have estimated the parameters from the literatures and done simulation through MATLAB. Here we have considered an example of spleen mouse given in table 1 [11]. We have considered the two

**Table 1.** Description of variables and parameters

Description	Variables/Parameters	Values
Population size of uninfected cells	$X_0$	$10^8$
Average life time of a cell infected with tachyzoites	$\frac{1}{a_T}$	18
Average life time of a cell infected with bradyzoites	$\frac{1}{a_C}$	240
Production rate of free parasite for tachyzoites	$k_T$	8/18
Production rate of free parasite for bradyzoites	$k_C$	1024/240
Removal rate of free parasite for tachyzoites	$u_T$	48
Rate constants	$\beta_T, \beta_B$	$8.889/10^{10}, 8.533/10^9$
Removal rate of free parasite for bradyzoites	$u_B$	20
Removal rate of the immune system response	$\delta$	1/48
Production rate of the effector cells	$\rho$	10/24
Half saturation constant	$h$	$10^5$
Rate of conversion of early-stage bradyzoites	$r_B$	1/48
Rate of conversion of Tachyzoites	$r_T$	1/108
Average life time of an uninfected cell	$d$	$1.389/10^3$

different cases for model 1(b). In first case we have assumed that there is no immune response and, in second case there is an active immune response. In model 1(b) we have considered logistic growth of healthy cells and no immune response with holding Type II functional response [Fig 3] as a rate of infection. It can be observed from the figure that number of healthy cells started decreasing gradually after infection and after a certain time interval again it started increasing [Fig 3(left)]. Population of the infected cells containing tachyzoites

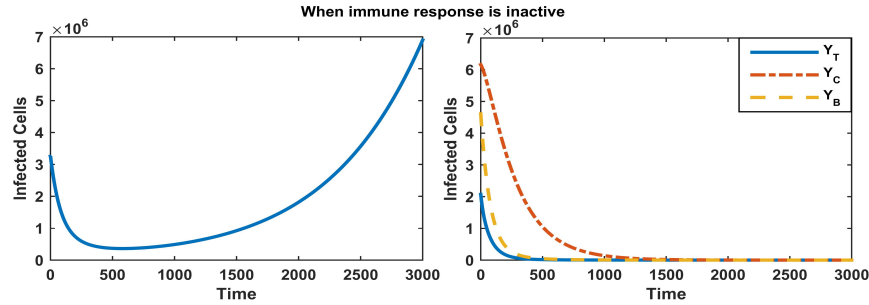


**Fig. 3.** Healthy cells (left) and infected cells (right) for model (1b) when immune response is absent

and encysted bradyzoites reduced sharply as compared to earlystage bradyzoites [Fig 3(right)]. When we considered active immune response then ob-

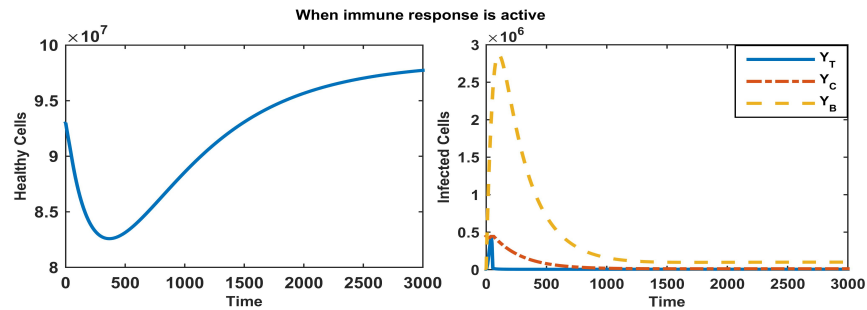


**Fig. 4.** Healthy cells (left) and infected cells (right) for model (1b) when immune response is present

served that number of healthy cells decreased for 450 seconds but after that it started increasing in the presence of active immune [Fig 4(left)]. Population of infected cells containing tachyzoites and early-stage bradyzoites reduced faster as compared to the cells containing encysted bradyzoites [Fig 4(right)]. Therefore, active immune response suppressed the infection due to *Toxoplasma gondii* for the holling type II functional response.

#### 4.1 Sensitivity Analysis

Sensitivity analysis of a model is tool to understand the response of parameters in transmission of disease. Also with the help of sensitivity analysis we can easily understand the importance of each parameter in the dynamics of the diseases. It helps researchers to estimate the date of parameters and also that parameter, which has high impact on reproduction number, equation (18). Changes in variables of model 1(b) after changing the values of parameter can be observed by sensitivity analysis. For the model 1(b) the reproduction

number is given by the equation (18). Sensitive index of reproduction number with respect to a given parameter is defined by [Eqn. 51] as follows:

$$\gamma_p^{R_0} = \frac{\partial R_0}{\partial p} \frac{p}{R_0} \tag{51}$$

Therefore, we have the following expression corresponding to each parameter which are associated with the expression of reproduction number:

$$\xi_1 = \gamma_{X_0}^{R_0} = \frac{\partial R_0}{\partial X_0} \frac{X_0}{R_0} = 1 \tag{52}$$

$$\xi_2 = \gamma_{\beta_T}^{R_0} = \frac{\partial R_0}{\partial \beta_T} \frac{\beta_T}{R_0} = \frac{a_C \beta_T}{(\beta_T a_C + \beta_B r_T)} \tag{53}$$

$$\xi_3 = \gamma_{\beta_B}^{R_0} = \frac{\partial R_0}{\partial \beta_B} \frac{\beta_B}{R_0} = \frac{r_T \beta_B}{(\beta_T a_C + \beta_B r_T)} \tag{54}$$

$$\xi_4 = \gamma_{a_C}^{R_0} = \frac{\partial R_0}{\partial a_C} \frac{a_C}{R_0} = -\frac{r_T \beta_B}{(\beta_T a_C + \beta_B r_T)} \tag{55}$$

$$\xi_5 = \gamma_{r_T}^{R_0} = \frac{\partial R_0}{\partial r_T} \frac{r_T}{R_0} = \frac{r_T (\beta_T a_C + r_T \beta_B + \beta_B a_T + \beta_B r_T)}{(\beta_T a_C + \beta_B r_T)(a_T + r_T)} \tag{56}$$

$$\xi_6 = \gamma_{a_T}^{R_0} = \frac{\partial R_0}{\partial a_T} \frac{a_T}{R_0} = \frac{a_T}{(a_T + r_T)} \tag{57}$$

We have evaluated the values of parameters, variables and sensitivity index of the model 1(b) using the equation (18) as reproduction number. We have calculated sensitivity index for each parameter associated in the expression of reproduction number which is given by equation (52 - 57). Sensitivity index is represented in the table (2).

**Table 2.** Parameters and its sensitivity index

Parameters	Values
$X_0$	1
$\beta_T$	0.0448
$\beta_B$	0.9552
$r_T$	1.0981
$a_T$	0.8571
$a_C$	-0.9552

Now we have analyzed the impact of parameters on the reproduction number of the given models and found that  $\beta_T$  is less sensitive as compared to other parameters. Here  $\gamma_{X_0}^{R_0} = 1$  that means when we increase or decrease  $X_0$  then with the same percentage it will impact on the reproduction number. We have increased the value of each parameter by  $\pm 5\%$  and  $\pm 10\%$  [Fig 5 - 7] and observed the dynamics of the T. Gondii and its infection corresponding to

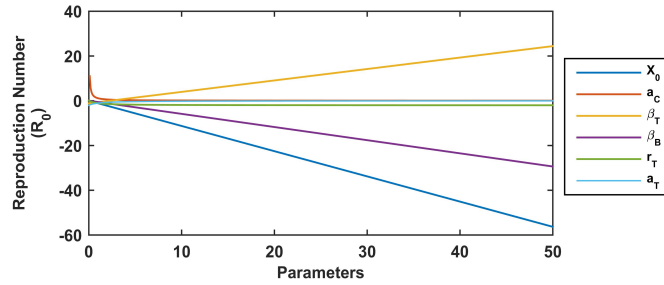


**Fig. 5.** Sensitivity analysis of parameters of the reproduction number

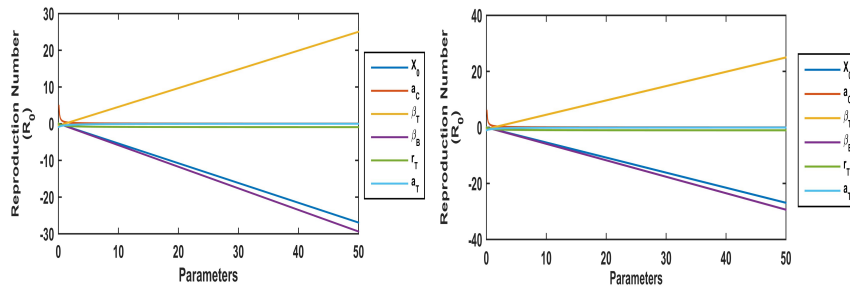


**Fig. 6.** Sensitivity analysis of parameters of the reproduction number when increased (left) and decreased (right) by 5%

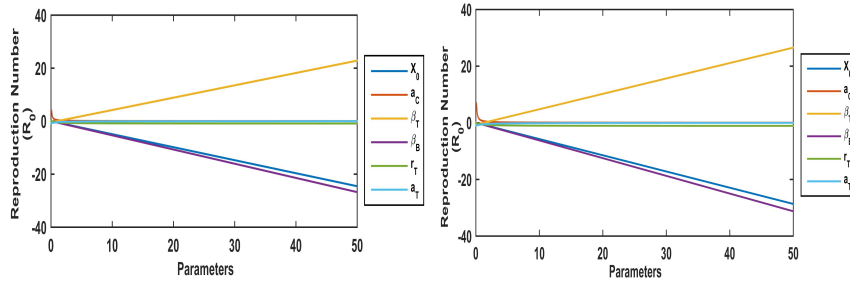


**Fig. 7.** Sensitivity analysis of parameters of the reproduction number when increased (left) and decreased (right) by 10%

the infected cells containing tachyzoites, early-stage bradyzoites and encysted bradyzoites. Now we have observed that for uninfected  $X_0$  at equilibrium point in the absence of immune response, population of infected cells containing tachyzoites and cells containing early-stage bradyzoites reduced faster as compared to population of cells containing encysted bradyzoites [Fig 8(left)]. Infected cells for the original value is dominated over all the infected cells of increased (black) and decreased (blue) for initial time interval and tend towards zero after 500 seconds. In the presence of active immune response, the number of infected cells containing tachyzoites and cells containing encysted bradyzoites tend towards zero with respect to time. It has been clearly ob-

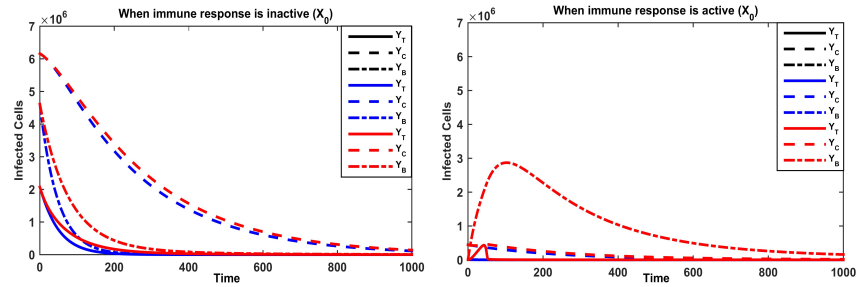


**Fig. 8.** Sensitivity analysis of parameter  $X_0$  of the reproduction number for both (left) inactive immune X response and (right) active immune response when parameter is increased (Black) and decreased (Blue) by 5% and compared with original (Red) value. Solid curve represents infection due to tachyzoites  $Y_T$ , dash-dot curve represents early-stage bradyzoites  $Y_B$ , and dash curve represents encysted bradyzoites  $Y_C$ .

served from the figure [Fig 8(right)] that the black and blue coloured infected cells reduced much faster than the red curve. This shows that dynamics is very sensitive towards the parameter  $X_0$ . Infection reduced much faster for the increased (black) and decreased (blue) value of uninfected cells by 5% as compared to original (red) value of parameter [Fig 8(right)]. In absence of immune

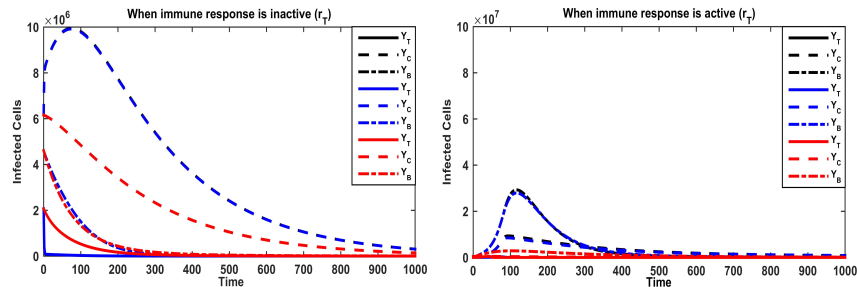


**Fig. 9.** Sensitivity analysis of parameter  $r_T$  of the reproduction number for both (left) inactive immune X response and (right) active immune response when parameter is increased (Black) and decreased (Blue) by 5% and compared with original (Red) value. Solid curve represents infection due to tachyzoites  $Y_T$ , dash-dot curve represents early-stage bradyzoites  $Y_B$ , and dash curve represents encysted bradyzoites  $Y_C$ .

response, the population of infected cells containing encysted bradyzoites reduced slower as compared to population of infected cells containing tachyzoites and cells containing early-stage bradyzoites [Fig 9(left)]. Infection for original (red) value of rate of conversion of Tachyzoites ( $r_T$ ) reduced faster as compared to increased (black) and decreased (blue) value of parameter. In the presence of active immune response, the number of infected cells containing tachyzoites reduced faster as compared to cells containing early-stage bradyzoites and en-

cysted bradyzoites with respect to time. It has been clearly observed from the figure [Fig 9(right)] that original (red) value of rate of conversion of tachyzoites ( $r_T$ ) reduced much faster than the increased (black) and decreased (blue) rate of conversion of tachyzoites. This shows that infection reduced much more for original (red) value of uninfected cells as compared to the decreased (blue) and the increased (black) value of rate of conversion of tachyzoites ( $r_T$ ) by 5% when immune response is considered as active for the system [Fig 9(right)]. We observed that the impact of rate constant  $\beta_T$  on the dynamics of the

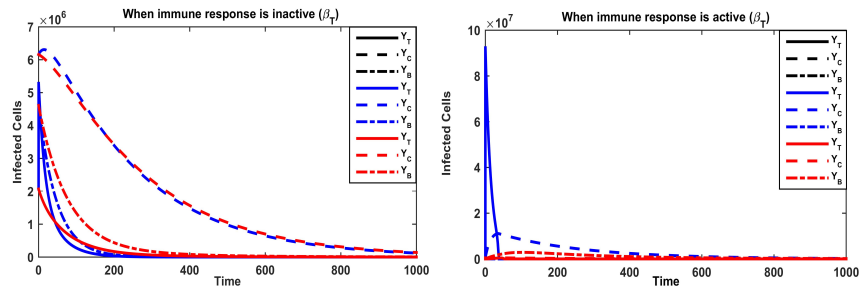


**Fig. 10.** Sensitivity analysis of  $\beta_T$  of the reproduction number for both (left) inactive immune X response and (right) active immune response when parameter is increased (Black) and decreased (Blue) by 5% and compared with original (Red) value. Solid curve represents infection due to tachyzoites  $Y_T$ , dash-dot curve represents early-stage bradyzoites  $Y_B$ , and dash curve represents encysted bradyzoites  $Y_C$ .

model 1(a). When immune response is considered inactive, then the infected cells containing encysted bradyzoites reduced slower as compared to cells containing tachyzoites and cells containing early-stage bradyzoites [Fig 10(left)]. For the cells containing encysted bradyzoites, original (red) value has almost some impact as compared to increased (black) and decreased (blue) value of  $\beta_T$  by 5%. But for the cells containing early-stage bradyzoites, original (red) value dominated over increased (black) and decreased (blue) value of rate constant  $\beta_T$ . For starting time interval up to 50 seconds, infected cells containing tachyzoites have higher values. But after the passage of time it reduced faster as compared to original (red) value for increased and decreased value of  $\beta_T$ . When we have considered active immune response, cells containing tachyzoites and encysted bradyzoites have higher value for starting time interval in the case of increased (black) and decreased (blue) value as compared to original (red) value of parameter  $\beta_T$  [Fig 10(right)]. But the infected cells containing early-stage bradyzoites tends towards zero faster for the increased (black) and decreased (blue) value by 5% than the original (red) value of parameter  $\beta_T$ . In the case of inactive immune response, the infected cells containing tachyzoites reduced very soon as compared to the cells containing encysted bradyzoites for increased (black) and decreased (blue) value as compared to original value of parameter  $a_T$  [Fig 11(left)]. For the population of cells containing early-stage bradyzoites dynamics are same for original (red), increased (black) and decreased (blue) of parameter  $a_T$ . However, the population of the cells contain-

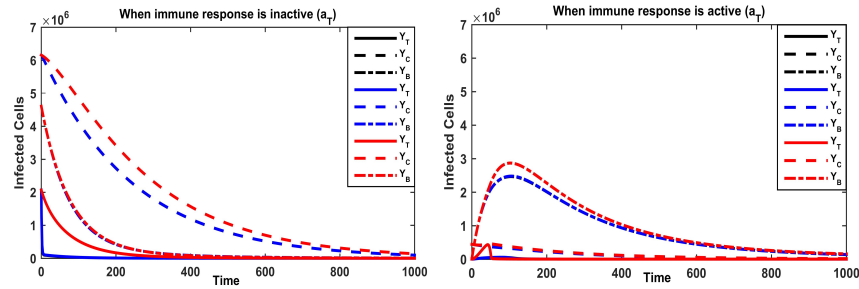


**Fig. 11.** Sensitivity analysis of parameter  $a_T$  of the reproduction number for both (left) inactive immune X response and (right) active immune response when parameter is increased (Black) and decreased (Blue) by 5% and compared with original (Red) value. Solid curve represents infection due to tachyzoites  $Y_T$ , dash-dot curve represents early-stage bradyzoites  $Y_B$ , and dash curve represents encysted bradyzoites  $Y_C$ .

ing encysted bradyzoites dominated for original value of parameter  $a_T$  up to 900 seconds and after that die out with respect to time. For the case of active immune response, the population of cells containing tachyzoites and encysted bradyzoites reduced faster as compared to the population of cells containing early-stage bradyzoites. Dynamics of the infections of *T. gondii* are almost same for increased (black), decreased (blue) by 5% and original (red) value of parameter  $a_T$  up to 80 seconds and after than original (red) value of infected cells dominated and again approached to the same after almost 600 seconds [Fig 11(right)].

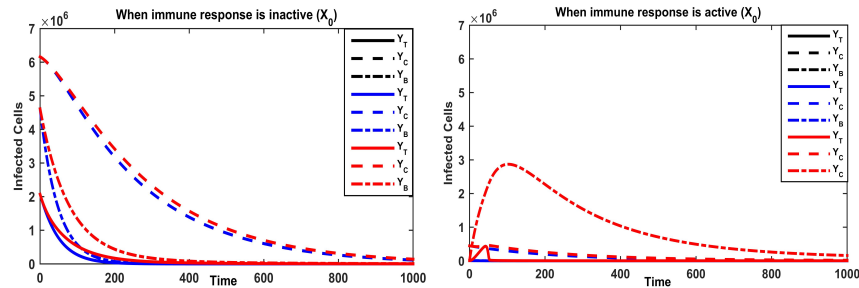


**Fig. 12.** Sensitivity analysis of parameter  $X_0$  of the reproduction number for both (left) inactive immune X response and (right) active immune response when parameter is increased (Black) and decreased (Blue) by 10% and compared with original (Red) value. Solid curve represents infection due to tachyzoites  $Y_T$ , dash-dot curve represents early-stage bradyzoites  $Y_B$ , and dash curve represents encysted bradyzoites  $Y_C$ .

Infection reduced in the case of inactive immune response much faster for the cells containing tachyzoites and cells containing early-stage bradyzoites for the increased (black) and decreased (blue) as compared to original (red) value

of parameter  $X_0$ . For infected cells containing encysted bradyzoites dynamic differ slightly after 100 seconds [Fig 12(left)]. But again, increased (black) and decreased (blue) value of parameter  $X_0$  by 10% approached to the same as original value after 800 seconds. When we have considered active immune response then we have observed the dominated dynamics of infected cells containing earlystage bradyzoites over the cells containing for original (red) values as compared to increased (black) and decreased (blue) value of parameter  $X_0$  by 10%. Infected cell containing tachyzoites to zero very quickly for the increased (black) and decreased (blue) of parameter by 10% and have same property for the infected cells containing encysted bradyzoites  $0 < X < 1$  [Fig 12(right)].

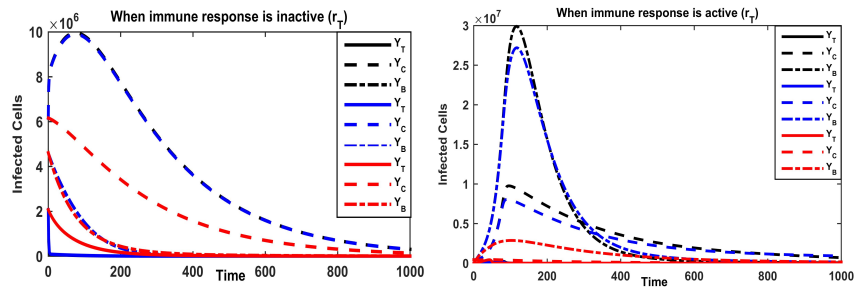


**Fig. 13.** Sensitivity analysis of parameter  $r_T$  of the reproduction number for both (left) inactive immune response and (right) active immune response when parameter is increased (Black) and decreased (Blue) by 10% and compared with original (Red) value. Solid curve represents infection due to tachyzoites  $Y_T$ , dash-dot curve represents early-stage bradyzoites  $Y_B$ , and dash curve represents encysted bradyzoites  $Y_C$ .

In case of inactive immune response, infected cells containing encysted bradyzoites have dominated dynamics for increased (black) and decreased (blue) value of rate of conversion of tachyzoites ( $r_T$ ) as compared to original value (red) [Fig 13(left)]. Infected cells containing early-stage bradyzoites have almost similar dynamics for all three cases-original (red), decreased (blue) and increased (black) value of rate of conversion of tachyzoites ( $r_T$ ). But for the infected cells containing tachyzoites reduces very quickly for increased (black) and decreased (blue) values of rate of conversion of tachyzoites ( $r_T$ ) by 10% as compared to original (red). When we considered active immune response, dynamics is very diverse and varying. Infected cells containing early-stage bradyzoites have similar behavior up to 80 seconds for increased (black) and decreased (blue) values of rate of conversion of tachyzoites ( $r_T$ ) but after 80 seconds infected cells for increased (black) value have higher peak than decreased (blue) value rate of conversion of tachyzoites ( $r_T$ ). But after 240 seconds again dynamics are same and changing after 300 seconds and lastly approached to zero for further time interval. For infected cells containing encysted bradyzoites have also same behavior up to 80 seconds and after that infected cells for increased (black) values dominated and again after 700 seconds it has same behavior as infected cells containing encysted bradyzoites for decreased (blue) values.

Infected cells containing encysted bradyzoites and tachyzoites reduced quickly towards zero original (red) value of rate of conversion of tachyzoites ( $r_T$ ) and also infected cells containing tachyzoites for increased (black) and decreased (blue) value of rate of conversion of tachyzoites ( $r_T$ ) goes towards zero very quickly [Fig 13(right)].

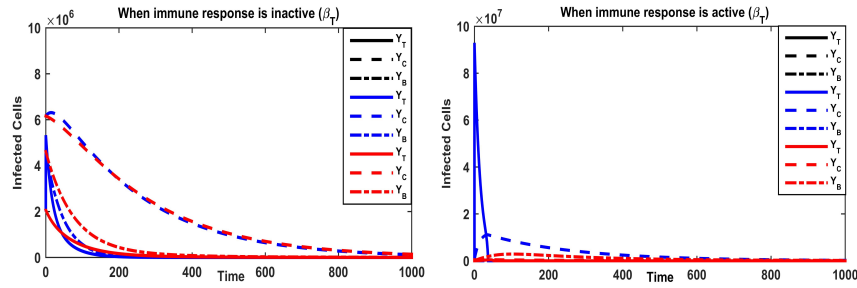


**Fig. 14.** Sensitivity analysis of parameter  $\beta_T$  of the reproduction number for both (left) inactive immune X response and (right) active immune response when parameter is increased (Black) and decreased (Blue) by 10% and compared with original (Red) value. Solid curve represents infection due to tachyzoites  $Y_T$ , dash-dot curve represents early-stage bradyzoites  $Y_B$ , and dash curve represents encysted bradyzoites  $Y_C$ .

We observed that the impact of parameter  $\beta_T$  on the dynamics of the model 1(b). When immune response is considered inactive, then the infected cells containing encysted bradyzoites reduced slower as compared to cells containing tachyzoites and cells containing early-stage bradyzoites [Fig 14(left)]. For the cells containing encysted bradyzoites, original (red) value has almost some impact as compared to increased (black) and decreased (blue) value of  $\beta_T$  by 10%. But for the cells containing early-stage bradyzoites, original (red) value dominated over increased (black) and decreased (blue) value of rate constant  $\beta_T$  [Fig 14(left)]. For starting time interval up to 50 seconds, infected cells containing tachyzoites have higher values. But after the passage of time it reduced faster as compared to original (red) value for increased and decreased value of  $\beta_T$ . For the active immune response, cells containing tachyzoites and encysted bradyzoites have higher value for starting time interval in the case of increased (black) and decreased (blue) value as compared to original (red) value of parameter  $\beta_T$  [Fig 14(right)]. But the infected cells containing early-stage bradyzoites tends towards zero faster for the increased (black) and decreased (blue) value by 10% than the original (red) value of parameter  $\beta_T$  [Fig 14(right)]. Firstly for the inactive immune response, the infected cells containing tachyzoites reduced very soon as compared to the cells containing encysted bradyzoites for increased (black) and decreased (blue) value as compared to original value of parameter  $a_T$ . For the population of cells containing early-stage bradyzoites dynamics are same for original (red), increased (black) and decreased (blue) of parameter  $a_T$  [Fig 15(left)]. However, the population of the cells containing encysted bradyzoites dominated for original value of parameter  $a_T$  up to 900

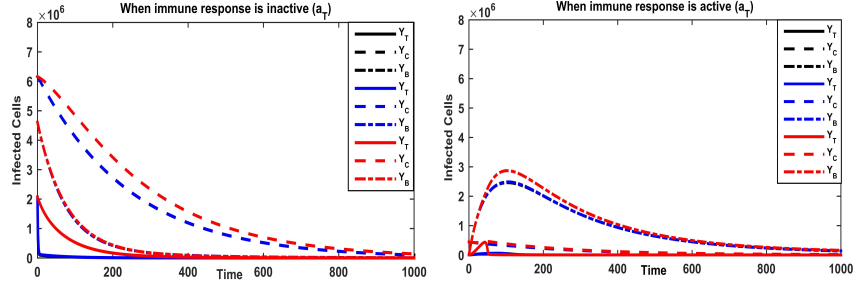


**Fig. 15.** Sensitivity analysis of parameter  $a_T$  of the reproduction number for both (left) inactive immune X response and (right) active immune response when parameter is increased (Black) and decreased (Blue) by 10% and compared with original (Red) value. Solid curve represents infection due to tachyzoites  $Y_T$ , dash-dot curve represents early-stage bradyzoites  $Y_B$ , and dash curve represents encysted bradyzoites  $Y_C$ .

seconds and after that die out with respect to time. When we have considered active immune response then observed that the population of cells containing tachyzoites and encysted bradyzoites reduced faster as compared to the population of cells containing early-stage bradyzoites. Almost same dynamics have been observed for the infections of *T. gondii* in the case of increased (black), decreased (blue) by 10% and original (red) value of parameter  $a_T$  up to 80 seconds and after than original (red) value of infected cells dominated and again approached to the same after almost 600 seconds [Fig 15(right)]. After analyzing all the aspects of parameters associate with reproduction number it has been concluded that  $\beta_T$  is less sensitive as compared to other parameters. Therefore other parameters associated with reproduction number are more effective than  $\beta_T$  to suppress infection due to tachyzoites  $Y_T$ , early-stage bradyzoites  $Y_B$ , encysted bradyzoites  $Y_C$ .

## 5 Discussion and Results

In this manuscript, we have proposed model for infection transmitted by a parasite- *Toxoplasma gondii*. Here we have assumed that there is conversion between bradyzoites and tachyzoites. Logistic growth of healthy cells has been considered and impact of immune responses has been analyzed on the dynamics of *Toxoplasma gondii*. We have also performed stability analysis for disease free equilibrium and endemic equilibrium for the proposed model. Also we have analyzed the sensitivity of parameters which has impact on reproduction number  $R_0$ .

- i. It has been found that for  $R_0 < 1$  model shows locally asymptotically stable disease-free equilibrium and unstable for  $R_0 > 1$ .
- ii. In the absence of immune response proposed model has a unique endemic equilibrium for  $R_0 > 1$  whereas in presence of active immune response model has a unique endemic equilibrium for  $R_0 > 1$  and  $\rho > \delta$ .

- iii. It has been analyzed that holding type II functional response play important role in supression of infection due to *Toxoplasma gondii*. Also the impact of immune responses reduced the population of infected cells as compared to inactive immune response.
- iv. The endemic equilibrium of the model (1b) is locally asymptotically stable in the absence of immune if  $R_0 < 1$ .
- v. The endemic equilibrium of the model (1b) is locally asymptotically stable in the presence of immune if  $R_0 < 1$  and  $\rho < \delta$ .
- vi. It has been concluded that  $\beta_T$  is less sensitive and therefore other parameters associated with reproduction number are more effective than  $\beta_T$  to suppress infection due to tachyzoites  $Y_T$ , early-stage bradyzoites  $Y_B$ , encysted bradyzoites  $Y_C$ .

Finally, numerical simulations have been done to support our mathematical work. We have considered both cases of active and inactive immune response and results justified that active immune response suppressed the infection within the hosts.

## 6 Acknowledgement

First author would like to acknowledge DST/INSPIRE/03/2016/000597 for financial support.

## References

1. Mimi Y. and Ruiqing S., Analysis of an SI Epidemic Model with Nonlinear Incidence Rate in an Environmentally-driven Infectious Disease, *British Journal of Mathematics & Computer Science*, 4(20): 2942-2953, 2014.
2. Maria J. G., Idalina F., Anabela V., Susana M., Carlos C., Susana S., Baltazar N., João P. G., *Toxoplasma gondii* seroprevalence in the Portuguese population: comparison of three cross sectional studies spanning three decades. *BMJ Open*, 6- e011648, 2016. DOI: 10.1136/bmjopen-2016-011648.
3. Annisa R., Barandi S. W., Mahardika A. W., and Wayan T. A., Prevalence and Risk Factors for Toxoplasmosis in Middle Java, Indonesia, *EcoHealth* 14, 162–170, 2017, DOI: 10.1007/s10393-016-1198-5.
4. Stepanova E. V., Kondrashin A. V., Sergiev V. P., Morozova L. F., Turbabina N. A., Maksimova M. S., Romanov D. V., Kinkulkina M. A., Lazareva A. V., Morozov E. N., Toxoplasmosis and mental disorders in the Russian Federation (with special reference to schizophrenia). *PLoS ONE* 14(7): e0219454, 2019. doi.org/10.1371/journal.pone.0219454
5. Tedford E. and McConkey G., Neurophysiological Changes Induced by Chronic *Toxoplasma gondii* Infection, *Pathogens*, 6,19, 2017, doi:10.3390/pathogens6020019
6. Alshehri H. M. , Almathami J. A., Alsumairi R. A., Binabdulrahman B. A., Nemenqani D. M., Soliman R. H., Association between *Toxoplasma gondii* and mental disorders in Taif region, *Saudi J Health Sci* 2019;8:42-6, 2019.
7. Berdoy M., Webster J. P., Macdonald D. W., Fatal attraction in rats infected with *Toxoplasma gondii*, *Proc Biol Sci.*, 267(1452):1591-4, 2000.

8. Stock A. K., Dajkic D., Kohling H. L., Heinegg E. H. V., Fiedler M. and Beste C., Humans with latent toxoplasmosis display altered reward modulation of cognitive control, *Scientific Reports*, 7, 10170, DOI:10.1038/s41598-017-10926-6.
9. Eells J. B., Varela-Stokes A., Guo-Ross S. X., Kummari E., Smith H. M., Cox E., Lindsay D. S., Chronic *Toxoplasma gondii* in *Nurr1*-null heterozygous mice exacerbates elevated open field activity, *PLoS One*, 10(4)-e0119280, 2015, doi: 10.1371/journal.pone.0119280.
10. Uttah E., Ogban E., and Okonofua C., Toxoplasmosis: A global infection, so widespread, so neglected, *International Journal of Scientific and Research Publications*, Volume 3, Issue 6, 1 ISSN 2250-3153, 2013.
11. Sullivan A., Agosto F., Bewick S., Su C., Lenhart S. and Zhao X., A Mathematical Model for within-host *Toxoplasma gondii* Invasion Dynamics, *Math Biosci Eng.* 9, 647-62, 2012.